Soil Biology and Biochemistry 206 (2025) 109801

Contents lists available at ScienceDirect

Soil Biology and Biochemistry

journal homepage: www.elsevier.com/locate/soilbio

Decoupling of heat and CO_2 release during decomposition of cellulose and its building blocks in soil

Fatemeh Dehghani [a,*], Thomas Reitz [a,b], Steffen Schlüter [c], Matthias Kästner [d], Evgenia Blagodatskaya [a]

[a] Helmholtz-Centre for Environmental Research – UFZ, Department of Soil Ecology, Theodor-Lieser-Str. 4, 06120, Halle (Saale), Germany
[b] Martin Luther University Halle-Wittenberg (MLU), Institute of Agricultural and Nutritional Sciences - Crop Research Unit, Julius-Kühn-Straße 23, 06112, Halle, Germany
[c] Helmholtz-Centre for Environmental Research – UFZ, Department of Soil System Science, Theodor-Lieser-Str. 4, 06120, Halle (Saale), Germany
[d] Helmholtz-Centre for Environmental Research – UFZ, Department of Molecular Environmental Biotechnology, Permoserstr. 15, 04318, Leipzig, Germany

ARTICLE INFO

Keywords:
Calorespirometry
Enthalpy
Depolymerization
Cellobiose
β-glucosidase
Cellobiohydrolase

ABSTRACT

The degradation of large biopolymers, such as cellulose, in soil requires several enzymatic hydrolysis steps to produce simpler substrates for microbial uptake. The synthesis of these enzymes requires energy and takes time until they are fully expressed. However, the heat release associated with enzymatic hydrolysis and the temporal delay between this initial heat release and the final carbon mineralization to CO_2 is largely unknown. In this study, we investigated the dynamics of heat and CO_2 release during the sequential decomposition of cellulose to its building blocks, cellobiose and glucose, in soil and related these processes to activities of cellobiohydrolase and β-glucosidase driving the corresponding steps of cellulose decomposition. Moreover, we estimated catabolic heat release during the stepwise enzymatic production of oligo- and monomers in soil by employing fluorogenically labeled substrates. This amounted to the absolute value of 26.5 kJ mol C^{-1}, approximately 6.5 % of the total combustion enthalpy stored in the applied cellulose.

By three complementary approaches, we confirmed that cellobiohydrolase rather than β-glucosidase is the bottleneck step of enzymatic hydrolysis. First, a 36 h temporal decoupling between the heat and CO_2 formation peaks occurred during step-wise enzymatic hydrolysis of cellulose performed by cellobiohydrolase and β-glucosidase towards final mineralization. This decoupling was not observed in the next sequential step of cellobiose hydrolysis by β-glucosidase. Remarkably, heat and CO_2 release evolved more slowly during cellulose degradation compared to that of its building blocks, cellobiose and glucose. Second, the enzyme activity of β-glucosidase more than doubled that of cellobiohydrolase during cellulose degradation. Third, heat release after the addition of flurogenically labeled substrate to soil, which mimics the steps of cellulose degradation, was faster in the step of glucose production than that of cellobiose production. This study highlights the novel mechanistic insights facilitated by calorespiroemetric monitoring of carbon decomposition at high temporal resolution.

1. Introduction

Carbon (C) storage in soil is a result of microbial processing of plant residues to be either transformed to high and low molecular weight compounds of soil organic matter (SOM) or respired as CO_2 due to mineralization processes. Soil microorganisms require organic compounds not only as a C source, but also as an energy source for growth, maintenance, and shifting from dormancy to activity (Lennon and Jones, 2011). They use these compounds to meet their growth needs by anabolism, as well as energy acquisition by catabolism (Kästner et al., 2024). In this context, the efficiency with which microorganisms retain metabolized C in their biomass, referred to as carbon use efficiency (CUE) (Geyer et al., 2016; Manzoni et al., 2018), and its energy counterpart, energy use efficiency (EUE) are interconnected to each other through energy channel from catabolic to anabolic processes. Therefore, measuring carbon and energy release jointly by calorespirometry can provide a more complete picture of metabolic pathways during matter

This article is part of a special issue entitled: Soil C and energy fluxes published in Soil Biology and Biochemistry.

* Corresponding author.
E-mail address: fatemeh.dehghani@ufz.de (F. Dehghani).

https://doi.org/10.1016/j.soilbio.2025.109801
Received 31 August 2024; Received in revised form 21 February 2025; Accepted 1 April 2025
Available online 2 April 2025

List of abbreviations:

CBH	cellobiohydrolase
BG	β-glucosidase
Phos	Phosphatase
MUF-CB	4-Methylumbelliferyl β-D-cellobioside
MUF-βglu	4-Methylumbelliferyl β-D-glucopyranoside
MUF-P:	4-Methylumbelliferyl phosphate

and energy turnover in soil (Barros et al., 2016).

Soil calorespirometry in the last decades has covered a range of decomposition studies from animal waste (Dziejowski, 1995) and organochlorine herbicides (Cheney et al., 1996) to pure organic compounds (Critter et al., 2001), simplifying the complexity of the system. Most calorespirometry studies on pure organic substances rely on one compound, either monomeric (Barros et al., 2010; Herrmann and Bölscher, 2015; Geyer et al., 2019; Endress et al., 2024) or polymeric (Wadsö, 1995, 2009), not focusing on the fact that long-chain polymeric compounds require sequential steps of decomposition driven by soil enzymes.

Cellulose is the most prevalent C-containing plant polymer that is available for degradation in soil, consisting of glucose monomers coupled by β-1,4 glycosidic bonds (Lynd et al., 2002). Cellulose is transformed by a sequence of degradation steps into its oligomeric and monomeric building blocks, cellobiose and glucose, which are finally mineralized inside microbial cells (Fig. 1). Large biopolymers can be consumed as a substrate by soil microorganisms only after they are depolymerized extracellularly (Schimel and Weintraub, 2003; Kästner et al., 2021). The complete breakdown of energy-rich polymeric cellulose to assimilable glucose and CO_2 requires three spatially and temporally distinct processes: (i) energy-consuming synthesis of enzymes (ii) extracellular enzyme-mediated hydrolysis, and (iii) intracellular metabolism. First, microorganisms need to produce extracellular enzymes in an intracellular process by utilizing a carbon source and the energy stored in adenosine triphosphate (ATP), the general energy currency of living cells (Lengeler et al., 1999). In the second step, extracellular depolymerization of cellulose to glucose requires a synergistic action of different hydrolytic enzymes before the microorganisms finally metabolize the glucose inside the cell (Fig. 1). These extracellular enzymes are classified as cellulases, which hydrolyze the β-glycosidic bonds by introducing water molecules into the polymer structure. Endoglucanases randomly cut the bonds in the amorphous region of cellulose, culminating in a series of cello-oligosaccharides with smaller chain lengths. Next, exoglucanase, also known as cellobiohydrolase (CBH), targets the ends of cello-oligosaccharides producing cellobiose. Thereafter, β-glucosidase (BG) catalyzes the hydrolysis of the β-glycosidic bond in cellobiose resulting in the production of monomeric glucose (Eveleigh, 1987; Lynd et al., 2002; Lakhundi et al., 2015). These monomers are then transported into the cell through the cell membrane and are metabolized intracellularly via glycolysis and the respiratory chain. CO_2 is released as the end product of the Krebs cycle and the protons and electrons are transferred to oxygen as the terminal electron acceptor in the respiration chain enabling cellular energy storage by synthesizing ATP (Lengeler et al., 1999; Voet and Voet, 2010).

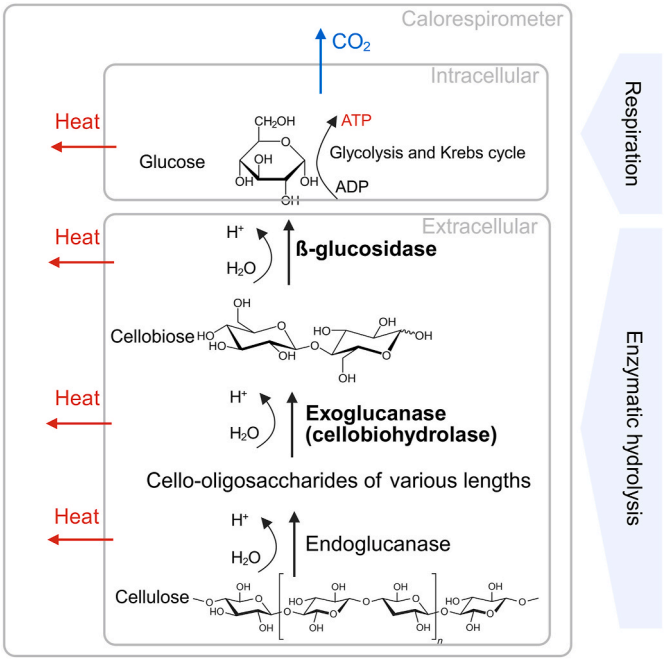

Fig. 1. Schematic figure depicting stages of cellulose degradation in soil comprising enzymatic hydrolysis and microbial respiration (mineralization).

Microbial respiration as well as growth- and maintenance-related processes are exothermic reactions that produce heat (Barros, 2021), which are the net outcome of simultaneous-occurring catabolic and anabolic reactions (Herrmann and Bölscher, 2015; Kästner et al., 2024). Microorganisms tend to utilize organic compounds only when the energy gain is higher than the demand for maintenance and sufficient for growth and enzyme production (Kästner et al., 2021). In the case of cellulose, on the one hand, synthesis and induction of cellulases is a metabolic burden for microorganisms (Lynd et al., 2002), on the other hand, the gain is an abundance of energy-rich, assimilable glucose. In addition, hydrolysis of the β-glycosidic bonds is energy-producing (Tewari and Goldberg, 1989; Sinnott, 1998; Brady et al., 2015; Sørensen et al., 2015). To what extent extracellular enzymatic hydrolysis contributes to the total metabolic heat release remains uncertain. It depends on the degree of polymerization of the cellulose, and calorimetry approaches cannot distinguish between the different contributions to overall heat release (red arrows in Fig. 1). To the best of our knowledge, there are no soil studies investigating the role of *in situ*-produced hydrolytic enzymes in the sequence of cellulose degradation steps and their contribution to heat release as well as the relation of heat and CO_2 formation. Therefore, it remains elusive whether extracellular heat formation by polymer hydrolysis may cause a temporal decoupling of heat and CO_2 formation. Moreover, it needs to be evaluated whether the extracellular heat formation depends on substrate complexity or is also affected by substrate quantity.

In this study, we focused on heat and CO_2 release in the course of two sequential decomposition stages of polymeric cellulose to oligomeric cellobiose and monomeric glucose in soil. The objectives of the study were (i) to unravel the dynamics of heat and CO_2 release during the decomposition of cellulose and its building blocks (oligomers and monomers), (ii) to relate matter and energy dynamics to the corresponding extracellular enzyme activities, and (iii) to compare the experimental values of CUE and EUE with the theoretical estimations for substrates with different levels of complexity. We applied isothermal microcalorimetry and respirometry techniques to monitor metabolic heat and CO_2 release during cellulose degradation for 14 days. To identify rate limitations in the cellulose degradation process, the degradation of its building blocks, cellobiose and glucose, was also monitored. In order to investigate microbial enzymes involved in the different stages of cellulose degradation, the activities of cellobiohydrolase (CBH) and β-glucosidase (BG) were determined during this process. Since standardized assays for the first step catalyzed by endoglucanase are missing, we studied only the last two steps of enzymatic hydrolysis in detail (Fig. 1). In addition, phosphatase (Phos) activity was determined as a proxy for the general microbial enzyme activity. To quantify the catabolic heat as a result of β-glycosidic bond cleavage, we sought to mimic the step-wise enzymatic breakdown of oligo- and

monomers. We added the corresponding fluorogenically labeled substrates commonly used in the enzyme assay to the soil for calorimetry measurements. This was done using the same experimental setup (soil amount, preincubation, moisture, etc) as for cellulose, cellobiose, and glucose. These fluorogenically-labeled substrates include 4-methylumbelliferyl β-D-cellobioside (MUF-CB; with 2 β-glycosidic bonds) which mimics the production of cellobiose from cellulose as well as 4-methylumbelliferyl β-D-glucopyranoside (MUF-βglu; with 1 β-glycosidic bond) imitating the production of glucose from cellobiose. Given that MUF is an organic compound, a control treatment is necessary to assess if MUF contributes to heat production. This approach helps to estimate the hydrolytic heat release as well as to identify the bottleneck step in the stages of cellulose degradation.

Based on the aforementioned reasonings, we hypothesized that (i) there will be a temporal decoupling between heat and CO_2 release for cellulose, in which the heat release preceded the CO_2 release, because the sequence of enzymatic break-down steps already releases heat, but only the final mineralization step yields CO_2 with the related metabolic heat. (ii) The time gap between the peak of heat and CO_2 release depends on the rate-limiting step and decreases with decreasing substrate complexity because fewer hydrolytic enzymes are required to mineralize simple organic substrate. (iii) The application of fluorogenically labeled substrates will be sensitive enough to estimate a net difference in heat release between two consecutive stages of cellulose degradation, through the hydrolysis of energy-yielding glycosidic bonds.

2. Material and methods

2.1. Experimental design

To investigate the first and second hypotheses, we performed incubation experiments using the substrates cellulose, cellobiose, and glucose. Both heat release and CO_2 evolution were measured for the samples. For more details see section 2.3.

To examine the third hypothesis, we assessed heat release after addition of fluorogenically-labeled substrates MUF-CB, MUF-βglu, as well as unlabeled glucose to the soil. For more details see section 2.5.

2.2. General soil characteristics and preincubation

Haplic Luvisol soils were collected in September 2021 at 0–20 cm depth from a long-term fertilization trial, initiated in 1904 at the Dikopshof experimental site of the University of Bonn, Germany. The trial includes a five-year crop rotation involving sugar beet, winter wheat, winter rye, legume (primarily Persian clover), and potato (oat until 1953). Since the establishment of the site, farmyard manure (5–12 t ha^{-1} yr^{-1}) was applied to the fertilized experimental plots, where the soil for the incubation experiment has been collected. Physico-chemical and biological characteristics of the soil are provided by (Lorenz et al., 2024).

The soil was air-dried, sieved through a 2 mm mesh, and homogenized. Prior to the incubation experiment, the soil was preincubated in a plastic tray at room temperature around 22 °C maintaining a gravimetric water content of 14 % for 10 days. This allowed to reestablish an active microbial community and let the immediate flush of microbial activity directly after rewetting pass. The tray was covered with aluminum foil, featuring a few holes to allow gas exchange while minimizing soil dehydration. Any seedlings grown during the preincubation time were immediately removed from the soil.

2.3. Respirometry and calorimetry

To test the first and second hypotheses, three carbon sources, cellulose (Isolife, Netherlands), cellobiose (Roth, Germany), and glucose (Chemsolute, Germany) were used for the study, whereby all were supplied homogeneously as a powder to the soil in incubation vessels. The cellulose from Isolife was ground using a ball mill (Retsch, Germany) comprised of a stainless steel cylinder and one ball of 1.5 cm diameter. The grinding was done with two consecutive runs (4 min, frequency of 30 s^{-1}). The cylinders were cooled at −20 °C for 5 min to avoid overheating by friction. This grinding step turned crystalline cellulose amorphous and changed the initial fluffy material into powder-like material which can be more easily distributed in the soil. The added carbon sources amounted to 1244 μg C g^{-1}, corresponding to ~8 times the microbial biomass carbon (MBC) content of the soil. Thereafter, soil water content was adjusted to 16 % (w/w) (52 % of WHC) by the addition of deionized water. Soil samples without substrate but only water addition were considered as the negative controls, to account for the effect of existing substrates in soil.

Heat release was monitored by an isothermal calorimeter (TAM Air, TA instruments, USA) in a twin configuration for soil and reference (water in amount ensuring equal heat capacity to soil sample). Heat flow rates (μW) were measured continuously at 20 °C. The rate of CO_2 efflux (mg CO_2 h^{-1}) was monitored in a respirometer (Respicond V, Sweden) via conductance changes of a KOH solution (10 ml, 0.6 M) induced by the absorption of CO_2 (Chapman, 1971; Nordgren, 1988).

Three replicates were used with 3.88 g and 34.11 g of dry soil per replicate in the 20 ml and 280 ml vials of TAM Air calorimeter and Respicond, respectively. The experimental setup maintained consistency across both the Respicond and TAM Air vials as the soil depth was set at approximately 0.9 cm in both cases. Additionally, a minimum ratio of 4:1 was established between the headspace volume and the soil volume in both container types to allow for sufficient aeration. The duration of each incubation was determined based on the observance of metabolic heat and CO_2 release. This period was 60 h for glucose and cellobiose, whereas it extended to 14 days for cellulose.

To investigate the effect of substrate amount on the dynamics of heat and CO_2, additional incubations were performed with cellulose (Roth, Germany) at 23 % (w/w) soil water content providing a range of substrate-C amounts of 800, 1600, and 3200 μg C g^{-1} corresponding to ~ 5, 10, 20 times of microbial biomass carbon (MBC) of the soil. All other conditions were similar to the main experiment.

In this study, we report the absolute values (modulus of value) of heat released during the observed microbial processes, irrespective of the fact that the heat flow was exothermic (by convention, heat release is considered to be negative).

2.4. Enzyme activity assessment

Extracellular enzyme activity of cellobiohydrolase, β-glucosidase, and phosphatase in the soil was measured on 5, 7, 11, and 14 days after cellulose addition using substrates artificially labeled with fluorogenic 4-methylumbelliferone (MUF) (Sigma-Aldrich, Germany). 4-methylumbelliferyl- β-D-cellobioside (CAS: 72626-61-0), 4-methylumbelliferyl-β-D-glucopyranoside (CAS:18997-57-4), and 4-methylumbelliferyl-phosphate (CAS: 3368-04-5) were applied for activity estimation of cellobiohydrolase (EC 3.2.1.91), β-glucosidase (EC 3.2.1.21), and phosphatase (EC 3.1.3.1), respectively. The rate of enzyme activity (υ in nmol g^{-1} h^{-1}) directly corresponds to the rate of 4-methylumbelliferon (4-MUF) release during the enzymatic reaction (Marx et al., 2001).

In short, 0.2 g (DW) soil was dispersed in 20 ml deionized water and sonicated for 1 min (40 J s^{-1}). Thereafter, 50 μl of the soil suspension and 50 μl of 0.1 M 4-morpholineethanesulfonic acid sodium (MES) buffer solution (pH 6.5) were transferred into a microplate. Afterwards, 100 μl of different dilutions of fluorogenic substrates were applied to the microplate wells, ensuring a range of 0–150 μM for phosphatase and 0–400 μM for cellobiohydrolase and β-glucosidase. The maximum concentration of the substrate for each enzyme was determined in a preliminary experiment where a saturation behavior was observed in enzymatic activity for different dilutions of the substrate. Microplates were incubated at room temperature in the dark, on a rotary shaker. Fluorescence was read by an Infinite 200 PRO instrument (Tecan Group

Ltd., Männedorf, Switzerland) with excitation and emission wavelengths of 360 nm and 465 nm at three time intervals after input of fluorogenically labeled substrate, (30 min, 90 min, and 150 min). The enzyme kinetic parameters, V_{max} and K_m were calculated according to the Michaelis-Menten equation:

$$\upsilon = \frac{V_{max} \times S}{K_m + S} \quad (1)$$

Where υ is the enzyme reaction rate (nmol g^{-1} h^{-1}), V_{max} is the maximum reaction rate (nmol g^{-1} h^{-1}), S is the substrate concentration (μM), and K_m is the half-saturation constant (μM).

2.5. Heat release after the addition of fluorogenically labeled substrates

The fluorogenically labeled substrates, 4-methylumbelliferyl-β-D-cellobioside (MUF-CB) and 4-methylumbelliferyl-β-D-glucopyranoside (MUF-βglu), that were used in the enzyme assay to study the release of cellobiose from cellulose and glucose from cellobiose, are associated with a specific heat release during the hydrolytic reaction. We further used these substrates as effective tools for estimating the heat of hydrolysis during the two sequential stages of cellulose degradation (third hypothesis). Importantly, cellobiohydrolase and β-glucosidase facilitate the direct reaction of cleaving a β-glycosidic bond in equimolar quantities and a synchronized manner. For this purpose, the fluorogenically labeled substrates 4-methylumbelliferyl-β-D-cellobioside (MUF-CB), 4-methylumbelliferyl β-D-glucopyranoside (MUF-βglu), and 4-methylumbelliferyl phosphate (MUF-phos) (Sigma-Aldrich, Germany) were dissolved in deionized water, 3 % (v/v) DMSO (dimethyl sulfoxide) to the concentration 10 mM. Thereafter, 400 μl of the substrates were added to already preincubated soil at a water content of 14 % in 20 ml vials of TAM Air calorimeter. The addition of the solution adjusted the final gravimetric soil moisture to 16 % as in the main experiment. An additional incubation was performed in which glucose solution with the same amount as MUF-substrates and the same concentration in water (equivalent to 74 μg C g^{-1}) was added to the soil. Heat flow (μW) was monitored for 45 h. Different negative controls were considered as soil amended with either water or MUF. All experiments were performed in triplicate.

2.6. DNA extraction and biomass determination

To determine the increment in microbial biomass carbon (MBC) of the soil during cellulose degradation, parallel soil incubations were performed in the same setting with the vial of TAM Air calorimeter. Here the increment in DNA was attributed to the increase in MBC of the soil by a conversion factor of f_{DNA} (Zheng et al., 2019) according to the following equation:

$$f_{DNA} = \frac{MBC_i}{DNA_i} \quad (2)$$

Where MBC_i is the initial amount of MBC in the soil used in the experiment amounted to 155 μg C g^{-1} (Lorenz et al., 2024) and DNA_i is the initial content of DNA in the soil amounted to 9.4 μg DNA g^{-1}.

For DNA extraction, 300 mg of fresh soil was collected on day 14 after cellulose addition to the soil. DNA was extracted using a modified version of the protocol of DNeasy PowerSoil Pro Kit (QIAGEN, Germany). The modification includes an additional homogenization to lyze the microbial cells. This was done using a homogenizer (Precelleys-24, PEQ-LAB, Germany) where the samples underwent homogenization at 5000 rpm in three batches each lasting 45s. DNA amount was quantified using a NanoDrop ND-8000 spectrophotometer (Thermo Fisher Scientific, Dreieich, Germany).

2.7. Carbon use efficiency (CUE) and energy use efficiency (EUE)

For the calculation of CUE and EUE, we applied different equations for cellulose as compared to cellobiose and glucose. This is justified by the fact that, unlike glucose and cellobiose, the complete mineralization of cellulose may not occur within the duration of the experiment. For cellobiose and glucose, we applied the equations of apparent CUE and EUE with the supposition of complete mineralization of substrates (Endress et al., 2024).

$$CUE = 1 - \frac{C_{CO2}}{C_s} \quad (3)$$

Where C_{CO2} denotes the cumulative C released as CO_2 after 60 h and C_s denotes the initially applied amount of C as cellobiose and glucose.

For cellulose, we used the following formula based on the amount of C incorporated into biomass and the total microbial C uptake (biomass formation and CO_2 evolution) (Sinsabaugh et al., 2013; Blagodatskaya et al., 2014a).

$$CUE = \frac{C_{biomass}}{C_{biomass} + C_{CO2}} \quad (4)$$

Where $C_{biomass}$ and C_{CO2} stand for the amount of C incorporated into biomass and C released as CO_2 up to day 14 after cellulose addition. This approach assumes that all C from the transformed cellulose was turned over to microbial biomass or CO_2 without any other product. The fraction of C utilized for synthesis of extracellular enzymes, for cellulose and cellobiose, is considered to be negligible for the aerobic soil (Manzoni et al., 2018). However, as we did not apply an isotopic approach here, we could not estimate the potential effects of positive priming; therefore, we will consider a potential underestimation of CUE in the discussion.

The energy use efficiency for cellobiose and glucose was calculated as:

$$EUE = 1 - \frac{Q}{\Delta H_s} \quad (5)$$

Where Q and ΔH_s represent the cumulative heat produced after 60 h of substrate addition and the combustion enthalpy of the substrates added (450 kJ C mol^{-1} and 468.9 kJ C mol^{-1} for cellobiose and glucose, respectively) (Gorokhov and Sryvalin, 1973).

For the EUE of cellulose degradation, with the same analogy of CUE, we consider only the part of the depolymerized cellulose that is either converted into microbial biomass or evolved as CO_2. This is necessary as cellulose is probably not completely degraded during 14 days. In this case, EUE is approximated by the thermodynamic enthalpy efficiency of soil microbial communities (η_{eff}) (Bölscher et al., 2016), an adapted version of equations proposed by (Battley, 1960; Harris et al., 2012), to relate the energy used for metabolism to the total energy consumed by microorganisms.

$$\eta_{eff} = 1 - \frac{Q}{Q_m} \quad (6)$$

Where Q_m denotes the energy metabolized by microorganisms and Q denotes the total heat released. Q_m can be calculated experimentally from the fraction of metabolized C ($\Delta MBC + \Delta CO_2$ = amount of substrate converted to biomass and CO_2) and the combustion enthalpy of the total substrate added (ΔH_s).

$$\eta_{eff} = 1 - \frac{Q}{(\Delta MBC + \Delta CO_2)^* \Delta H_s} \quad (7)$$

Combustion enthalpy of the ground isolife cellulose was measured to 15.01 kJ g^{-1} (Lorenz et al., 2024), which is at the lower level for amorphous celluloses measured in the literature (Goldberg et al., 2015). For the sake of simplicity in this paper, we refer to the thermodynamic

enthalpy efficiency of soil microbial communities (η_{eff}) as energy use efficiency (EUE).

2.8. Data and statistical analysis

CO_2 and heat release curves of cellulose and its control were smoothed by applying a combination of a 5h-moving median to remove the outliers and a 24 or 72-h moving average (depending on the extent of noises) to reduce noise in the signal.

Total heat and CO_2 (cumulative values) were calculated by integrating the rates of heat and CO_2 over the incubation period as following

$$Q\,(t) = \int_{t=0}^{t} P(t)dt \tag{8}$$

$$C\,(t) = \int_{t=0}^{t} CER(t)dt \tag{9}$$

where Q and P stand for cumulative heat (J) and heat flow rate (W) also C and CER for cumulative CO_2 evolution (mg CO_2) and CO_2 evolution rate (mg CO_2 h^{-1}).

Heat flow after the addition of fluorogenically labeled substrates (μW g^{-1}) was normalized per metabolizable C in the structure of MUF-CB and MUF-βglu so the C in the MUF structure was excluded as it did not contribute to the heat release (see results in Fig. 5a). For the structures of the fluorogenic substrates see Fig. S1.

Mass and energy balance equations for the complete mineralization of three substrate-C applied in our study (hypotheses 1 and 2) are indicated by the following chemical equations:

$$\text{Cellulose} \rightarrow CO_2 + \text{Biomass} + \text{metabolic heat} + \text{hydrolysis heat} \tag{10}$$

$$\text{Cellobiose} \rightarrow CO_2 + \text{Biomass} + \text{metabolic heat} + \text{hydrolysis heat} \tag{11}$$

$$\text{Glucose} \rightarrow CO_2 + \text{Biomass} + \text{metabolic heat} \tag{12}$$

These equations represent the sequential steps of cellulose degradation. To address the difference in degradation timescales between cellulose (weeks to months) and cellobiose as well as gluocse (hours to days), we employed fluorogenically labeled substrates. This approach enabled us to synchronize substrate degradation and standardize the molarity of added C. For the estimation of hydrolytic heat release (hypothesis 3), the energy balance for each fluorogenic substrate was expressed using the following equations:

$$\text{MUF-CB} \rightarrow dH_1 + \text{dH-priming} \tag{13}$$

$$\text{MUF-βglu} \rightarrow dH_2 + \text{dH-priming} \tag{14}$$

$$\text{Glucose} \rightarrow dH_3 + \text{dH-priming} \tag{15}$$

Where dH_1, dH_2, and dH_3 represent the heat released due to metabolic use of MUF-CB, MUF-βglu, and glucose, respectively. Hydrolytic heat release from degradation of cellulose to cellobiose can be quantified as dH_1 - dH_2. Likewise, hydrolytic heat release from degradation of cellobiose to glucose amounts to dH_2 - dH_3.

We suppose that heat release due to soil priming will be similar for all fluorogenic labeled substrates. This assumption is valid since soil priming is linked to the amount of C added. The priming effect is relatively small when the amount of C added is around or less than soil MBC, which was the case of fluorogenic substrates added (74 μg C g^{-1} of glucose and MUF-βglu as well as 148 μg C g^{-1} of MUF-CB with soil MBC 155 μg C g^{-1}). In addition, the experimental timeframe (45 h) usually corresponds with zero to negative priming due to the triggering effect compensated by preferential substrate utilization (Blagodatskaya and Kuzyakov, 2008).

Normalized enzyme activities were determined by the ratio of averaged V_{max} values in cellulose-amended soil and non-amended soil. The standard deviation was calculated by the propagation of the error. The enzyme kinetics parameters were calculated via a non-linear curve fitting by OriginPro software (2022b). The schematic figure (Fig. 1) was created by BioRender.

3. Results

3.1. CO_2 and heat dynamics for different substrates

In the cellulose-amended soil, microbial growth started only after approximately two days of incubation with clear peaks in heat and CO_2 release at 4.7 and 6.2 days after cellulose addition, respectively (Fig. 2a). A clear temporal decoupling of heat and CO_2 curves was observed, not only during peak emissions but also during the exponential growth phase (Fig. 2a). The peak of heat release roughly aligned with the steepest ascending slope of CO_2 release. In contrast, CO_2 and heat release from non-amended soil remained at a baseline value throughout the whole incubation, where small fluctuations in the heat signal were at the detection level of the device. This indicates that the effect of native substrate existing in the soil on substrate-induced heat and CO_2 was negligible.

The heat and CO_2 curves of glucose and cellobiose treatments were quite synchronous during the ascending growth phase and peaked between 19 and 23 h after substrate addition, with ~ 2h earlier peaks for glucose compared to cellobiose (Fig. 2b and c). The curves of cellulose treatment leveled off gradually to the baseline value. In contrast, in the case of cellobiose and glucose, the decrease in metabolic curves was sharper within ~3h after the peak time which turned into a plateau followed by a gradual decreasing rate.

3.2. Enzyme activity

In the cellulose-amended soil, the hydrolytic reaction mediated by β-glucosidase was on average ~2.5 times faster than that of cellobiohydrolase (Fig. 3a). The normalized enzyme activity (ratio of cellulose-amended and non-amended soil) showed values larger than 1 for CBH and BG, which indicates an increased level of all cellulases secreted by microorganisms to break down cellulose into glucose (Fig. 3b). CBH activity strongly increased to a variable extent over time, and was 2.5, 3.1, 4.9, and 3.9 times higher than that of non-amended soil after 5, 7, 11, and 14 days, respectively (Fig. 3b). In contrast, BG activity only increased slightly but more equally in the course of incubation (average factor: 1.5), while Phos activity did not show any significant variation from the activity measured in non-amended soil. Interestingly, after cellulose addition, K_m increased only in the case of CBH and not for BG and Phos on an average basis of all sampling days, indicating a decreased affinity of CBH towards cellulose, which is presumably caused by the growth of other degrading organisms and the induction of CBH with different properties (Fig. 3c).

3.3. Effect of initial C amount added on the delay time

By increasing the amount of cellulose from 5 × MBC to 10 × MBC, both heat and CO_2 curves peaked at an earlier time, however, the time shift was larger for CO_2 than for heat, which reduced the gap between the heat and CO_2 peak (Fig. 4). Specifically, the peak time shifted from day 8.9 to 6.8 for CO_2 and from day 7.1 to 6.2 for heat. Interestingly, by further increasing the amount of substrate to 20 times MBC, CO_2 curves preceded that of heat, that is, day 4.6 and 5.2 for CO_2 and heat respectively.

3.4. Heat release of fluorogenic substrates

A clear metabolic heat peak was observed after the addition of MUF-CB, MUF-βglu, and glucose to the soil, but not by the addition of MUF

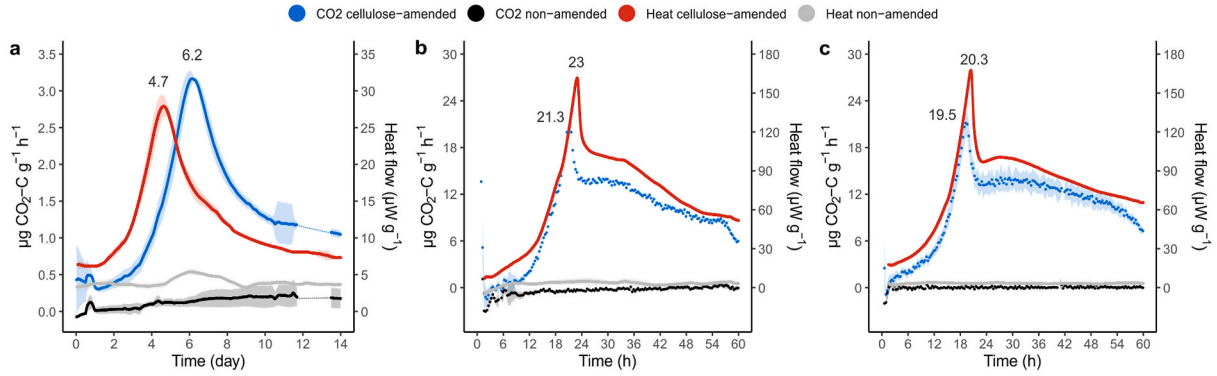

Fig. 2. Rate of CO_2 and heat release in the course of degradation of (a) cellulose during 14 days (b) cellobiose during 60 h and (c) glucose during 60 h. Substrate addition amounted to 1244 μg C g^{-1}, corresponding to ~ eight times of microbial biomass C (MBC) content of the soil. The experiments were performed at 16 % gravimetric soil moisture and 20 °C. For all treatments, absolute values of heat release are illustrated. Data are the average values of three or four replicates. Shadows represent 95% confidence intervals.

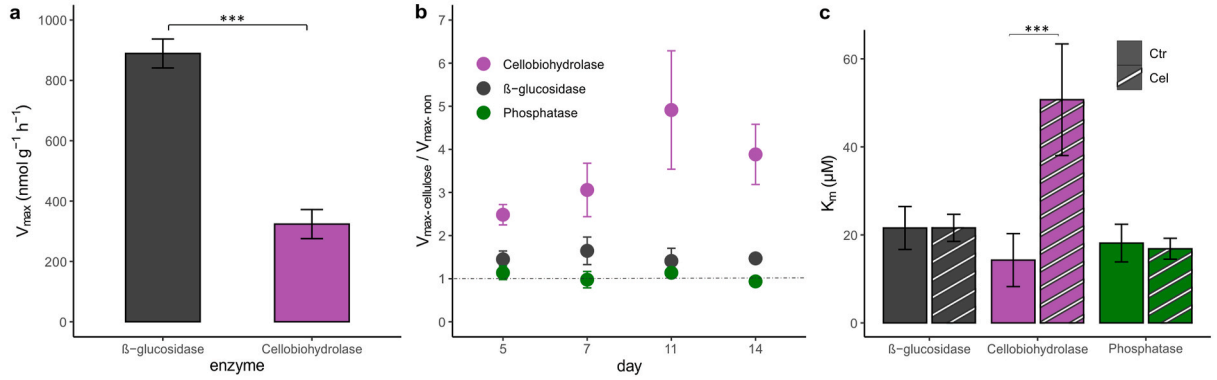

Fig. 3. Kinetics of extracellular enzymes during degradation of cellulose in soil (a) average values of 4 sampling days for enzyme activity (V_{max}) of β-glucosidase and cellobiohydrolase during 14 days after cellulose addition to the soil. (b) dynamics of normalized enzyme activity ($V_{max\text{-}cellulose}/V_{max\text{-}non}$) of cellobiohydrolase, β-glucosidase, and phosphatase. The points are the average values of 4 replicates (c) average value of 4 sampling days for half-saturation constants (K_m) of cellobiohydrolase, β-glucosidase, and phosphatase during 14 days of cellulose addition to the soil. Simple and patterned bars denote non-amended and cellulose-amended soil. Bars represent 95% confidence intervals.

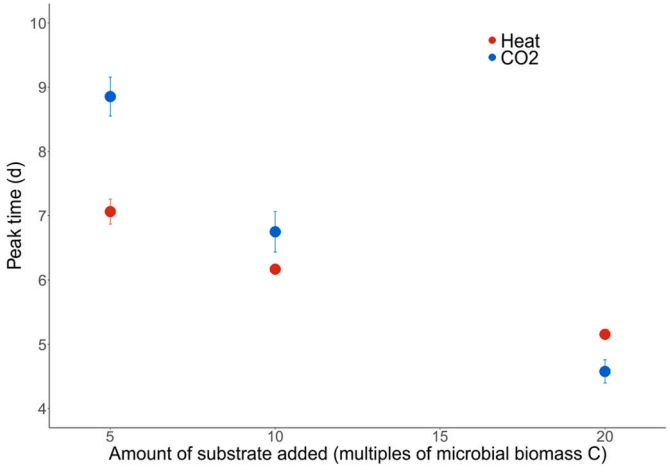

Fig. 4. The time of peak in heat and CO_2 curves (different colors) for different amounts of cellulose added based on soil MBC at 20 °C and 23 % gravimetric soil moisture. Bars represent 95% confidence intervals. (For interpretation of the references to color in this figure legend, the reader is referred to the Web version of this article.)

(Fig. 5a) and MUF-Phos (Fig. S2). This indicates that MUF itself was not cleaved during the time frame of our experiment and did not contribute to the heat development. The dynamics of heat release were gauged by the time when 50 % of the total heat during 45 h was released (points in Fig. 5a). These time points corresponded to 9.4, 13, and 16.5 h for glucose, MUF-βglu, and MUF-CB, respectively (Fig. 5a). For the same molar concentration of glucose, MUF-βglu showed a delayed and extended peak compared to that of glucose (Fig. 5a). During 45 h, the cumulative heat release amounted to 1.04 J g^{-1} (4.035 J) for MUF-βglu and 2.4 J g^{-1} (9.312 J) for MUF-CB addition. Normalized heat release per metabolizable C provides strong evidence (p-value = 0.004) for a higher heat release from metabolizing MUF-CB (0.194 J μmol C^{-1}) than MUF-βglu (0.168 J μmol C^{-1}) (Fig. 5b). Similar cumulative normalized heat release was detected in glucose and MUF-βglu treatments (Fig. 5b) at the end of the incubation (after 45 h) even though glucose peaked earlier than MUF-βglu (Fig. 5a).

4. Discussion

4.1. Cellobiohydrolase as the rate-limiting step during cellulose degradation in soil

In accordance with the first hypothesis, a distinct 36 h temporal decoupling between the peaks of heat and CO_2 release was observed in the course of cellulose decomposition in soil. In contrast, heat and CO_2

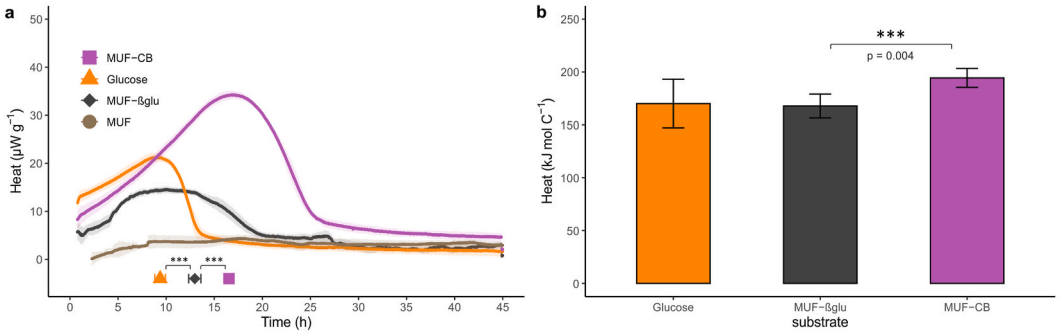

Fig. 5. Heat release after the addition of fluorogenically labeled substrates to the soil, 4-Methylumbelliferyl-β-D-cellobioside (MUF-CB), 4-Methylumbelliferyl-β-D-glucopyranoside (MUF-βglu), 4-Methylumbelliferron (MUF), and glucose. (a) Rate of heat release (subtracted from respective negative controls) by the addition of MUF-CB, MUF-βglu, MUF, and glucose. Points represent the time when 50 % of total heat (during 45 h) is released. (b) Cumulative heat release normalized per metabolizable-C added at the end of the incubation (45 h) for the treatments with a clear peak, i.e. treatments amended with MUF-CB, MUF-βglu, and glucose. For all treatments, absolute values of heat release are illustrated. Shadows and bars represent 95% confidence intervals.

curves were tightly coupled during the decomposition and metabolic use of cellobiose and especially glucose (Fig. 2). Cellulose, cellobiose, and glucose generally have similar chemical structures and only differ in their degree of linear polymerization by β-1,4 glycosidic bonds formed via condensation reactions with the release of water (Lengeler et al., 1999). These compounds have a similar nominal oxidation state of carbon (NOSC) of zero, which may be the highest energy gain for microorganisms using oxygen as a terminal electron acceptor (LaRowe and Van Cappellen, 2011). These compounds also have similar energy content considering the combustion enthalpy ($\Delta_c H$). For example, $\Delta_c H°$ (25 °C) values for cellobiose and glucose amount to 450 kJ C mol^{-1} and 468.9 kJ C mol^{-1}, respectively (Gorokhov and Sryvalin, 1973) and other sources give 418 kJ mol^{-1} C for amorphous cellulose (Goldberg et al., 2015). Therefore, the dynamical differences in heat and CO_2 release may result from the polymer properties of cellulose, which need to be degraded enzymatically by extracellular enzymes.

Complete mineralization of cellulose to CO_2 includes extracellular enzyme hydrolysis and intracellular metabolism of glucose. Hydrolytic reactions *per se* do not produce CO_2 and are low energy-releasing catalytic reactions (Voet and Voet, 2010). The energy produced outside the cell by hydrolysis of the biopolymer will be released as heat since it does not generate electron transfers in microbial metabolism and thus cannot be used to generate ATP (Lengeler et al., 1999). CO_2 will be released only during intracellular metabolism when the monomeric glucose passes through the cell membrane to be oxidized to CO_2 through cellular catabolism and respiration. This step produces both heat, as the part of energy that is not utilizable, and CO_2, as the end product of the Krebs cycle. This was observed in the case of glucose as the sole substrate added (Fig. 2c). All these steps occurred simultaneously, so the CO_2 and heat release are not necessarily separated in time (Fig. 2a). In particular, in our experiment, heat and CO_2 were not measured from the same soil sample. Nevertheless, the experimental setup (detailed in section 2.3) was designed to minimize any potential inconsistencies between the two measurements. It is worth mentioning that we observed a small delay between CO_2 formation and detection in the experiments, but critically any diffusion constraints leading to a CO_2 delay are ruled out by the fact that these reasons would evoke a fixed offset for all substrates and substrate amounts, which was not the case in our study (see Fig. 4). Moreover, such diffusion constraints may only take less than 2 h in the respirometry setup (Endress et al., 2024).

In line with our second hypothesis, with decreasing substrate complexity the delay time between heat and CO_2 release was also reduced (Fig. 2). The different decomposition dynamics of the three tested substrates, gauged by peak times in the range of 4.7–6.2 days, 21.3–23 h, and 19.5–23 h for cellulose, cellobiose, and glucose, as well as two times slower reaction mediated by CBH as compared with BG (Fig. 3a) provided complementary confirmation that the bottleneck step between the two sequential stages of cellulose degradation is the production of cellobiose through hydrolysis by CBH and not the cleavage of cellobiose by β-glucosidases. The limitation can be even more intense as the total activity of β-glucosidase might have been underestimated. This is because not all the β-glucosidase is extracellular and bacteria can degrade cellobiose also by intracellular β-glucosidase activity (Wilson, 2008).

Although the rate of enzyme activity in cellulose-amended soil was more than two times smaller for cellobiohydrolase than β-glucosidase (Fig. 3a), the overall increase of enzymatic activity after cellulose addition (expressed as normalized enzyme activity: V_{max} cellulose-amended soil/V_{max} non-amended soil) was on average two times higher for cellobiohydrolase than for β-glucosidase (Fig. 3b). This explains that, in comparison to the more constitutive levels of BG and Phos, cellulose addition strongly stimulated induction and synthesis of CBH, the activity of which is normally lower than BG activity in soil without addition of cellulose (Loeppmann et al., 2016; Breitkreuz et al., 2021). Hence, microorganisms possibly compensate for lower activity of CBH by synthesizing it at a higher level. The normalized enzyme activity of CBH did not drop immediately after the decrease in respiration starting at day 6.2 (Fig. 2a), but it increased to day 7 with a peak at day 11 and dropped on day 14 (Fig. 3b). Likewise, the normalized enzyme activity of BG stayed constant even after the time of maximum heat and CO_2 release. This legacy effect is explained either by the stability of enzymes activity in the soil even one month after substrate addition (Renella et al., 2007; Blagodatskaya and Kuzyakov, 2013) perhaps through attachment of cellulases to microbial cells (Wilson, 2008; Yan and Wu, 2013) or by the continuation of enzyme production by microorganisms to maintain their activity as long as sufficient substrate and energy flux is provided. This is plausible considering that enzymes synthesized to fulfill a particular resource demand may remain functional even when the demand is no longer present (Allison et al., 2007; Burns et al., 2013). Interestingly by cellulose addition, K_m increased significantly only for CBH and not for BG and Phos (Fig. 3c). This implies either the growth of a more diverse microbial community or a higher variety of enzymes comprising other kinetic properties for the cleavage of cellobiose from cellulose.

The slower leveling off in the heat and CO_2 rates after the peak time in cellobiose and glucose incubation as compared to cellulose incubation suggests a potential nutrient limitation for microbes in the latter treatments (Fig. 2). Due to the faster uptake and turnover, it is perhaps plausible that the amount of carbon added surpassed the amount of nutrients in the soil, as the soil was not amended with an additional nutrient solution. Under these conditions, soil microorganisms cannot utilize all of the available C during the exponential growth phase. They keep metabolizing the C source even after the exponential growth phase (Endress et al., 2024), either to perform overflow respiration and heat

release (Russell and Cook, 1995; Mooshammer et al., 2014; Chakrawal et al., 2022) to be ready for the occasional substrate input or to mine nutrients from soil organic matter (Moorhead and Sinsabaugh, 2006).

Notably, we observed that the temporal decoupling between heat and CO_2 formation was shortened from approximately 39 h to 16 h by increasing the amount of substrate from 5 to 10 multiples of MBC (Fig. 4). Elevated amounts of cellulose may accelerate microbial activation and growth, and thereby accelerate the whole process of enzymatic hydrolysis and intracellular metabolism of glucose (Fig. 1). The same trend was observed when the C addition was increased further to 20 multiples of times MBC, where interestingly even heat curve lagged behind the CO_2 curve (Fig. 4, Fig. S3). Such a large excess of the initial substrate (cellulose) provided large amounts of labile cellobiose and glucose. Under these conditions, it is plausible that microorganisms may shift their metabolism with the release of other presumably fermentation metabolites (Helling et al., 1987; Bernal et al., 2016) and may reduce their exoenzyme production until they utilize the more labile C-sources other than the not-yet-degraded biopolymer. Therefore, the "cheaters" may take advantage of the assimilable compounds produced outside the cell by "producers" (Allison, 2005). This may culminate in increased intracellular metabolism and an earlier complete mineralization to CO_2.

The delay in the exponential increase of heat and CO_2 in the first days after cellulose addition (Fig. 2a) was due to the re-allocation of C and energy resources for the synthesis and secretion of inducible extracellular enzymes to break down the polymeric chains of cellulose (Blagodatskaya et al., 2014b; Ramin and Allison, 2019). This delay was reduced for cellobiose and glucose with quite similar dynamics only differing in CO_2 and heat peaks. The small time difference between the heat peaks (~2h) after glucose and cellobiose addition may be attributed to the additional synthesis and secretion of β-glucosidases to cleave the β-glycosidic bond. This effect was more pronounced in a Cambisol preincubated with a nutrient solution and amended with fewer amounts of glucose and cellobiose (~400 μg C g^{-1}) in which ~ 6 h time difference for the heat peak between glucose and cellobiose was observed (Ropelewska et al., 2016). A similar trend was observed by comparing the dynamics of heat release after the addition of glucose and MUF-βglu, in which 50 % of the total heat release was achieved after 9.4 and 13 h, respectively (Fig. 5a). This is because microbial utilization of MUF-βglu requires the release of glucose by breaking the bonds between MUF and glucose before consumption. In other words, the starting point of the substrate decomposition is presumably a bit delayed, as in the MUF-βglu treatment the glucose was continuously produced in small amounts after the cleavage of the glycosidic bond in the structure of MUF-βglu by β-glucosidase in response to substrate input. The delay of the microbial growth phase after the addition of MUF-βglu indicates an energy burden on the microorganisms, as they need time and energy to produce additional extracellular enzymes to cleave the β-glycosidic bond. This energy could otherwise be directly used for growth (Manzoni et al., 2021) which was observed as immediate growth on glucose (Fig. 5a). This indicates that the degradation of compounds requiring extracellular enzymes for cleavage may cause a delay in time. Although this is beyond the scope of this study, future work is required to model the individual steps of cellulose degradation considering the temporal difference between the steps of cellulose degradation.

4.2. Heat of hydrolysis

In particular, we were able to quantify *in situ* hydrolytic heat released by cleavage of β-glycosidic bonds in the soil at the step of cellulose degradation to oligomers like cellobiose and relate its contribution to the total energy incorporated in the cellulose. The production of cellobiose and glucose was simulated with MUF-CB and MUF-βglu, which acted as the substrates for the enzymes CBH and BG. While the difference in total heat released between MUF-βglu and glucose treatments was not significant (Fig. 5b), an essential difference in total heat released at the end of the incubation (45 h) between MUF-CB and MUF-βglu treatments accounted for the value of 26.5 kJ mol C^{-1} (disregarding the negative sign), corresponding to 6.5 % of the combustion enthalpy of cellulose (15.01 kJ g cellulose^{-1} equivalent to 405.62 kJ mol C^{-1}). Remarkably, no significant heat release was observed in both the MUF and MUF-P treatments (Fig. 5a and Fig. S1). This confirms that consumption and thus the metabolic heat detected in MUF-βglu and MUF-CB treatments originated from the overall heat production of the sum of extracellular cleavage as well as the decomposition of MUF-cleaved glucopuranoside and cellobioside. The difference in heat release between the MUF-CB and MUF-βglu normalized per metabolizable C must account for processes other than microbial anabolism and catabolism resulting in microbial growth that are already included in both curves of MUF-CB and MUF-βglu. We assume, therefore, that this difference in metabolic heat was attributed to the hydrolytic cleavage of β-glycosidic bonds during cellobiose production by CBH. When expressed per mole of β-glycosidic bond (or mole of cellobiose, as each cellobiose contains one β-glycosidic bond), the estimated hydrolysis heat release was equivalent to the value of 318 kJ mol^{-1} cellobiose. This value is more than two orders of magnitude higher than the absolute value of *in vitro* ΔH of cellobiose hydrolysis (2.43 kJ mol^{-1} cellobiose) reported by (Tewari and Goldberg, 1989; Tewari et al., 2008). This is perhaps plausible considering that the *in vitro* experiment (Tewari and Goldberg, 1989) was performed for 1–2 h in a liquid solution under equilibrium conditions with just the addition of both substrates and enzymes. In contrast, our experiments were performed in native soil with living organisms lasting for 45 h. We expect that heat release in soil is dependent on specific soil properties that are absent in liquid media such as higher diversity of microbial communities, the presence of nutrients and additional substrates which may enhance microbial activity and heat production. However, we expect that this effect would be similar for all substrates as they were added in small and equimolar amounts. Thus, the heat exceeding the literature value may result from *in vivo* microbial turnover.

Notably, identical heat release in glucose and MUF-βglu treatments but greater heat release for MUF-CB indicates that the bond between the MUF and the sugar may not be as strong as the glycosidic bond in the cellobiose structure (for the structure of MUF-substrates see Fig. S1). In summary, we could quantify the hydrolytic heat during the extracellular step of cellobiose production from cellulose, thus partly confirming our last hypothesis. However, we were not able to quantify the hydrolysis heat for the step of cellobiose degradation to glucose in soil, as it might not have exceeded the detection limit of the device.

4.3. Carbon and energy balance: carbon and energy use efficiency (CUE and EUE)

Carbon and energy balances for cellulose indicated that after 14 days of cellulose addition, 32 % of the C added was released as CO_2. However, only 23 % of the total energy ($\Delta_c H^\circ$) contained in cellulose was released as heat (Table 1). For cellobiose and glucose after 60 h of incubation, these values equaled 45 % and 29 % as well as 46 % and 32 % (Table 1). Consistent for all three substrates, more C is released as CO_2 in comparison to the heat release. This implies that C is used in other processes than directly coupled catabolism and growth, such as formation of storage compounds (Mason-Jones et al., 2023), overflow metabolism, or other products, e.g. acetate, with much less heat release (Hansen et al., 2004; Bernal et al., 2016). It may even indicate the assimilation of biomass building blocks from SOM (Kästner et al., 2024). In addition, it implies that C, and presumably also heat, was released from other sources than cellulose, due to positive priming of SOM (Blagodatskaya et al., 2014b), when amending the soil with a large amount of C (~8 times MBC). Although the application of isotope labeling can confirm this for C, as recently proved for a cellulose incubation in the same soil by (Wirsching et al., 2025), detailed energy budgeting is not feasible with the current knowledge.

Table 1
Carbon and energy budgeting. The amount of energy added is calculated based on the absolute values of combustion enthalpy (Δ_cH) for the tested substrates:, Δ_cH° (glucose) = 468.9 kJ C mol^{-1}, Δ_cH° (cellobiose) = 450 kJ C mol^{-1} (Gorokhov and Sryvalin, 1973), Δ_cH° (cellulose) = 15.01 kJ g $cellulose^{-1}$ equivalent to 405.62 kJ mol C^{-1} (Lorenz et al., 2024).

Substrate type	Parameter	The amount added per soil g	The amount released per soil g	Percentage of released	Biomass per soil g	CUE
Cellulose	Carbon	1244 μg	398.12 ± 17 μg	32 %	73.25 ± 25.11 μg	0.15 ± 0.04
	Energy	42.44 J	9.85 ± 0.65 J	23 %		0.39 ± 0.03
Cellobiose	Carbon	1244 μg	580.77 ± 6.45 μg	45 %	NA	0.55 ± 0.00
	Energy	46.65 J	13.75 ± 0.03 J	29 %		0.70 ± 0.00
Glucose	Carbon	1244 μg	570.51 ± 6.45 μg	46 %	NA	0.54 ± 0.00
	Energy	48.61 J	15.40 ± 0.22 J	32 %		0.68 ± 0.00

The values of CUE and EUE for glucose and cellobiose were 0.54 and 0.55 as well as 0.68 and 0.70, respectively. This indicates that EUE values are larger than CUE values which are in line with the current finding for glucose (Endress et al., 2024) and in disagreement with the findings of (Wang and Kuzyakov, 2023). The potential CUE and EUE values for glucose and cellobiose calculated by the theoretical model of microbial turnover to biomass (MTB) (Brock et al., 2017; Trapp et al., 2018) were 0.43 and 0.47, respectively (for the detailed calculation see SI). As a pathway-independent approach, MTB applies the Gibbs energy release of the turnover reaction (ΔG) related to the microbially available electrons for calculating the potential biomass formation (yield) from substrate turnover under the relevant electron acceptor conditions. The inconsistency between experimental and theoretical CUE and EUE values indicates a possible overestimation of these parameters by the experimental approach and may indicate assimilation of other substrates from SOM. This is plausible considering the assumption that all substrates were metabolically consumed (see section 2.7). However, estimations using the MTB model predicted actual turnover values of <70 % for glucose and cellobiose and <60 % for cellulose based on the amount of C released as CO_2 within the experimental time frame. For cellulose, CUE and EUE values based on the metabolized part of depolymerized cellulose (CO_2 evolution and biomass formation) corresponded to only 0.15 and 0.39. Although both experimental values of CUE and EUE in our study were lower than the corresponding theoretical values predicted by the MTB model of 0.42 and 0.48, the difference was much larger for CUE compared to EUE. This may be due to a sudden decrease in microbial biomass, e.g., due to potential protozoan grazing observed on the 7th day of cellulose decomposition (Blagodatskaya et al., 2014b) or viral lysis. Moreover, while DNA is one of the most reliable proxies to determine microbial biomass content of the soil (Blagodatskaya et al., 2003; Malik et al., 2015; Čapek et al., 2023), the application of a constant factor for the conversion of DNA to biomass may lead to an underestimation of biomass during microbial growth. This is plausible because, after substrate addition, the ratio between microbial biomass and DNA content, i.e. f_{DNA}, tends to decrease during growth (Čapek et al., 2023). This is possibly due to a higher level of C use for formation of storage compounds (Mason-Jones et al., 2023) than for synthesizing DNA initially after substrate input.

Notably, the MTB model considers an average value of potential growth yield (Y), defined as biomass formed as a result of substrate mineralization, for estimating CUE and EUE. Moreover, the MTB approach is based on the release of Gibbs energy (ΔG) of the microbial turnover reaction including the respective electron acceptor (in this case oxygen), which indicates the feasibility and extent of microbial growth reactions and the potential microbial yields. In contrast, the EUE based on thermodynamic enthalpy efficiency (η_{eff}) takes into consideration the total actual changes in combustion enthalpy of the reaction (Δ_cH), which represents the heat released by combustion with oxygen at constant pressure that can be measured experimentally. The absolute values of Δ_cG are slightly higher than those of Δ_cH as ΔG contains the entropic contribution of the energy as well ($\Delta G = \Delta H\text{-}T\Delta S$) (Sandler and Orbey, 1991). The theoretical values derived from Gibbs energy change provide the upper limit for the assessment of microbial growth and turnover in the experimental results and indicate incomplete turnover of the supplied substrates in the present experiments. Therefore, the initial assumption of complete substrate turnover when calculating the amount of substrate supplied resulted in overestimation by the observed CUE and EUE compared to theoretical values of CUE and EUE. In any case, for the real C and energy assessment, information about the residual amount of substrate at the end of the incubation and turnover calculations would have been necessary. Overall, the observed discrepancy between the experimental and theoretical values of CUE and EUE, as predicted by the MTB model shows that the calculation of these parameters is highly method-dependent. This is particularly evident when the values derived using the apparent definition of these parameters (for glucose and cellobiose) exceeded the theoretical values, whereas, for cellulose, the experimental values based on metabolized C were lower than the theoretical predictions. This underscores the critical need to establish a standardized methodology for calculating CUE and EUE to ensure consistency and accuracy across various studies and contexts.

5. Conclusion

This study highlights the intricate relationship between mass and energy flows in the course of the complex microbial metabolism of cellulose and its building blocks in soil. For simple substrates like glucose and cellobiose, there is a close coupling between CO_2 release and heat production during microbial metabolism. However, for more complex substrates like cellulose, we observed a temporal decoupling between heat release and CO_2 production, suggesting that unaccounted energy sources, such as heat released during extracellular enzymatic hydrolysis, may play an additional significant role in the overall energy dynamics of cellulose degradation.

The observed decoupling emphasizes the need for process-based modeling that considers the sequential steps of cellulose degradation. Such models should account for the stepwise nature of cellulose breakdown, where the product of each enzymatic step becomes the substrate for the next. Furthermore, they should relate the rates of individual enzyme reactions to substrate consumption and product formation, while also considering the potential heat release from extracellular hydrolysis and its contribution to overall energy dynamics.

This study highlights the importance of considering the role of hydrolytic enzymes in calorespirometry studies, especially for polymeric compounds like cellulose, and provides a framework for developing more sophisticated C-cycling models that account for complex compounds and the enzyme-driven microbial processes in the soil environment.

CRediT authorship contribution statement

Fatemeh Dehghani: Writing – original draft, Visualization, Methodology, Investigation, Formal analysis, Data curation, Conceptualization. **Thomas Reitz:** Writing – review & editing, Supervision, Funding acquisition, Conceptualization. **Steffen Schlüter:** Writing – review & editing, Supervision, Funding acquisition, Conceptualization. **Matthias Kästner:** Writing – review & editing, Conceptualization, Methodology. **Evgenia Blagodatskaya:** Writing – review & editing, Supervision, Funding acquisition, Conceptualization, Methodology.

Data availability statement

The data used in this study are available upon request.

Declaration of competing interest

The authors declare that they have no known competing financial interests or personal relationships that could have appeared to influence the work reported in this paper.

Acknowledgments

This work was conducted within the framework of the priority program 2322 “SoilSystems”, funded by the German Research Foundation (DFG) under the grant of 465122443 (FD, TR, SS, EB), and TH 678/25-2 (MK). Soils were provided by S.J. Seidel and H. Hüging, University of Bonn, Germany. Soil characteristics were determined within the Priority Program 2322 “SoilSystems”.

Appendix A. Supplementary data

Supplementary data to this article can be found online at https://doi.org/10.1016/j.soilbio.2025.109801.

References

Allison, S.D., 2005. Cheaters, diffusion and nutrients constrain decomposition by microbial enzymes in spatially structured environments. Ecology Letters 8, 626–635. https://doi.org/10.1111/j.1461-0248.2005.00756.x.

Allison, V.J., Condron, L.M., Peltzer, D.A., Richardson, S.J., Turner, B.L., 2007. Changes in enzyme activities and soil microbial community composition along carbon and nutrient gradients at the Franz Josef chronosequence, New Zealand. Soil Biology and Biochemistry 39, 1770–1781. https://doi.org/10.1016/j.soilbio.2007.02.006.

Barros, N., 2021. Thermodynamics of soil microbial metabolism: applications and functions. Applied Sciences. https://doi.org/10.3390/app11114962.

Barros, N., Hansen, L.D., Piñeiro, V., Pérez-Cruzado, C., Villanueva, M., Proupín, J., Rodríguez-Añón, J.A., 2016. Factors influencing the calorespirometric ratios of soil microbial metabolism. Soil Biology and Biochemistry 92, 221–229. https://doi.org/10.1016/j.soilbio.2015.10.007.

Barros, N., Salgado, J., Rodríguez-Añón, J.A., Proupín, J., Villanueva, M., Hansen, L.D., 2010. Calorimetric approach to metabolic carbon conversion efficiency in soils: comparison of experimental and theoretical models. Journal of Thermal Analysis and Calorimetry 99, 771–777. https://doi.org/10.1007/s10973-010-0673-4.

Battley, E.H., 1960. Enthalpy changes accompanying the growth of Saccharomyces cerevisiae (hansen). Physiologia Plantarum 13, 628–640. https://doi.org/10.1111/j.1399-3054.1960.tb08085.x.

Bernal, V., Castaño-Cerezo, S., Cánovas, M., 2016. Acetate metabolism regulation in Escherichia coli: carbon overflow, pathogenicity, and beyond. Applied Microbiology and Biotechnology. https://doi.org/10.1007/s00253-016-7832-x.

Blagodatskaya, E., Blagodatsky, S., Anderson, T.-H., 2003. Quantitative isolation of microbial DNA from different types of soils of natural and agricultural ecosystems. Microbiology 72, 744–749. https://doi.org/10.1023/B:MICI.0000008379.63620.7b.

Blagodatskaya, E., Blagodatsky, S., Anderson, T.H., Kuzyakov, Y., 2014a. Microbial growth and carbon use efficiency in the rhizosphere and root-free soil. PLoS One 9. https://doi.org/10.1371/journal.pone.0093282.

Blagodatskaya, E., Khomyakov, N., Myachina, O., Bogomolova, I., Blagodatsky, S., Kuzyakov, Y., 2014b. Microbial interactions affect sources of priming induced by cellulose. Soil Biology and Biochemistry 74, 39–49. https://doi.org/10.1016/j.soilbio.2014.02.017.

Blagodatskaya, E., Kuzyakov, Y., 2013. Active microorganisms in soil: critical review of estimation criteria and approaches. Soil Biology and Biochemistry 67, 192–211. https://doi.org/10.1016/j.soilbio.2013.08.024.

Blagodatskaya, E., Kuzyakov, Y., 2008. Mechanisms of real and apparent priming effects and their dependence on soil microbial biomass and community structure: critical review. Biology and Fertility of Soils. https://doi.org/10.1007/s00374-008-0334-y.

Bölscher, T., Wadsö, L., Börjesson, G., Herrmann, A.M., 2016. Differences in substrate use efficiency: impacts of microbial community composition, land use management, and substrate complexity. Biology and Fertility of Soils 52, 547–559. https://doi.org/10.1007/s00374-016-1097-5.

Brady, S.K., Sreelatha, S., Feng, Y., Chundawat, S.P.S., Lang, M.J., 2015. Cellobiohydrolase 1 from Trichoderma reesei degrades cellulose in single cellobiose steps. Nature Communications 6. https://doi.org/10.1038/ncomms10149.

Breitkreuz, C., Heintz-Buschart, A., Buscot, F., Wahdan, S.F.M., Tarkka, M., Reitz, T., 2021. Can we estimate functionality of soil microbial communities from structure-derived predictions? A reality test in agricultural soils. Microbiology Spectrum 9. https://doi.org/10.1128/spectrum.00278-21.

Brock, A.L., Kästner, M., Trapp, S., 2017. Microbial growth yield estimates from thermodynamics and its importance for degradation of pesticides and formation of biogenic non-extractable residues. SAR and QSAR in Environmental Research 28, 629–650. https://doi.org/10.1080/1062936x.2017.1365762.

Burns, R.G., DeForest, J.L., Marxsen, J., Sinsabaugh, R., Stromberger, M.E., Wallenstein, M.D., Weintraub, M.N., Zoppini, A., 2013. Soil enzymes in a changing environment: current knowledge and future directions. Soil Biology and Biochemistry. https://doi.org/10.1016/j.soilbio.2012.11.009.

Čapek, P., Choma, M., Kaštovská, E., Tahovská, K., Glanville, H.C., Šantrůčková, H., 2023. Revisiting soil microbial biomass: considering changes in composition with growth rate. Soil Biology and Biochemistry 184. https://doi.org/10.1016/j.soilbio.2023.109103.

Chakrawal, A., Calabrese, S., Herrmann, A.M., Manzoni, S., 2022. Interacting bioenergetic and stoichiometric controls on microbial growth. Frontiers in Microbiology 13. https://doi.org/10.3389/fmicb.2022.859063.

Chapman, S.B., 1971. A simple conductimetric soil respirometer for field use. Oikos 22, 348. https://doi.org/10.2307/3543857.

Cheney, M.A., Sposito, G., McGrath, A.E., Criddle, R.S., 1996. Abiotic degradation of 2,4-D (dichlorophenoxyacetic acid) on synthetic birnessite: a calorespirometric method. Colloids and Surfaces A: Physicochemical and Engineering Aspects 107, 131–140. https://doi.org/10.1016/0927-7757(95)03385-8.

Critter, S.A.M., Freitas, S.S., Airoldi, C., 2001. Calorimetry versus respirometry for the monitoring of microbial activity in a tropical soil. Applied Soil Ecology 18, 217–227. https://doi.org/10.1016/S0929-1393(01)00166-4.

Dziejowski, J.E., 1995. Calorimetric and respirometric characteristics of the decomposition of animal wastewaters in soil. Thermochimica Acta 251, 37–43. https://doi.org/10.1016/0040-6031(94)02061-R.

Endress, M.-G., Dehghani, F., Blagodatsky, S., Reitz, T., Schlüter, S., Blagodatskaya, E., 2024. Spatial substrate heterogeneity limits microbial growth as revealed by the joint experimental quantification and modeling of carbon and heat fluxes. Soil Biology and Biochemistry 197, 109509. https://doi.org/10.1016/j.soilbio.2024.109509.

Eveleigh, D.E., 1987. Cellulase: a perspective. Philosophical Transactions of the Royal Society of London - Series A: Mathematical and Physical Sciences 321, 435–447. https://doi.org/10.1098/rsta.1987.0021.

Geyer, K.M., Dijkstra, P., Sinsabaugh, R., Frey, S.D., 2019. Clarifying the interpretation of carbon use efficiency in soil through methods comparison. Soil Biology and Biochemistry 128, 79–88. https://doi.org/10.1016/j.soilbio.2018.09.036.

Geyer, K.M., Kyker-Snowman, E., Grandy, A.S., Frey, S.D., 2016. Microbial carbon use efficiency: accounting for population, community, and ecosystem-scale controls over the fate of metabolized organic matter. Biogeochemistry 127, 173–188. https://doi.org/10.1007/s10533-016-0191-y.

Goldberg, R.N., Schliesser, J., Mittal, A., Decker, S.R., Santos, A.F.L.O.M., Freitas, V.L.S., Urbas, A., Lang, B.E., Heiss, C., Ribeiro Da Silva, M.D.M.C., Woodfield, B.F., Katahira, R., Wang, W., Johnson, D.K., 2015. A thermodynamic investigation of the cellulose allomorphs: cellulose(am), cellulose Iβ(cr), cellulose II(cr), and cellulose III (cr). Journal of Chemical Thermodynamics 81, 184–226. https://doi.org/10.1016/j.jct.2014.09.006.

Gorokhov, G.I., Sryvalin, I.T., 1973. Determination of the enthalpy of hydrolysis of carbohydrates from a homologous series of glucose. Izv. Vyssh. Uchebn. Zaved. Khim. Khim. Tekhnol. 16, 43–45.

Hansen, L.D., MacFarlane, C., McKinnon, N., Smith, B.N., Criddle, R.S., 2004. Use of calorespirometric ratios, heat per CO 2 and heat per O 2, to quantify metabolic paths and energetics of growing cells. In: Thermochimica Acta, pp. 55–61. https://doi.org/10.1016/j.tca.2004.05.033.

Harris, J.A., Ritz, K., Coucheney, E., Grice, S.M., Lerch, T.Z., Pawlett, M., Herrmann, A. M., 2012. The thermodynamic efficiency of soil microbial communities subject to long-term stress is lower than those under conventional input regimes. Soil Biology and Biochemistry 47, 149–157. https://doi.org/10.1016/j.soilbio.2011.12.017.

Helling, R.B., Vargas, C.N., Adams, J., 1987. Evolution of Escherichia coli during growth in a constant environment. Genetics 116, 349–358. https://doi.org/10.1093/genetics/116.3.349.

Herrmann, A.M., Bölscher, T., 2015. Simultaneous screening of microbial energetics and CO2 respiration in soil samples from different ecosystems. Soil Biology and Biochemistry 83, 88–92. https://doi.org/10.1016/j.soilbio.2015.01.020.

Kästner, M., Maskow, T., Miltner, A., Lorenz, M., Thiele-Bruhn, S., 2024. Assessing energy fluxes and carbon use in soil as controlled by microbial activity - a thermodynamic perspective A perspective paper. Soil Biology and Biochemistry 193, 109403. https://doi.org/10.1016/j.soilbio.2024.109403.

Kästner, M., Miltner, A., Thiele-Bruhn, S., Liang, C., 2021. Microbial necromass in soils—linking microbes to soil processes and carbon turnover. Frontiers in Environmental Science. https://doi.org/10.3389/fenvs.2021.756378.

Lakhundi, S., Siddiqui, R., Khan, N.A., 2015. Cellulose degradation: a therapeutic strategy in the improved treatment of Acanthamoeba infections. Parasites & Vectors. https://doi.org/10.1186/s13071-015-0642-7.

LaRowe, D.E., Van Cappellen, P., 2011. Degradation of natural organic matter: a thermodynamic analysis. Geochimica et Cosmochimica Acta 75, 2030–2042. https://doi.org/10.1016/j.gca.2011.01.020.

Lengeler, J.W., Drews, G., Schlegel, H.G., 1999. Biology of the Prokaryotes. John Wiley & Sons.

Lennon, J.T., Jones, S.E., 2011. Microbial seed banks: the ecological and evolutionary implications of dormancy. Nature Reviews Microbiology. https://doi.org/10.1038/nrmicro2504.

Loeppmann, S., Blagodatskaya, E., Pausch, J., Kuzyakov, Y., 2016. Substrate quality affects kinetics and catalytic efficiency of exo-enzymes in rhizosphere and detritusphere. Soil Biology and Biochemistry 92, 111–118. https://doi.org/10.1016/j.soilbio.2015.09.020.

Lorenz, M., Blagodatskaya, E., Finn, D., Fricke, C., Hüging, H., Kandeler, E., Kaiser, K., Kästner, M., Lechtenfeld, O., Marhan, S., Maskow, T., Mayer, J., Miltner, A., Normant-Saremba, M., Poll, C., Resseguier, C., Rupp, A., Schrumpf, M., Schweitzer, K., Simon, C., Tebbe, C., Yang, S., Yousaf, U., Thiele-Bruhn, S., 2024. Database for the priority program 2322 SoilSystems – soils and substrates used in the first phase (2021-2024). Zenodo v1, 1–5. https://doi.org/10.5281/zenodo.11207501 [Data set].

Lynd, L.R., Weimer, P.J., van Zyl, W.H., Pretorius, I.S., 2002. Microbial cellulose utilization: fundamentals and biotechnology. Microbiology and Molecular Biology Reviews 66, 506–577. https://doi.org/10.1128/mmbr.66.3.506-577.2002.

Malik, A.A., Dannert, H., Griffiths, R.I., Thomson, B.C., Gleixner, G., 2015. Rhizosphere bacterial carbon turnover is higher in nucleic acids than membrane lipids: implications for understanding soil carbon cycling. Frontiers in Microbiology 6. https://doi.org/10.3389/fmicb.2015.00268.

Manzoni, S., Čapek, P., Porada, P., Thurner, M., Winterdahl, M., Beer, C., Brüchert, V., Frouz, J., Herrmann, A.M., Lyon, S.W., Santruckova, H., Vico, G., Way, D., 2018. Reviews and syntheses: carbon use efficiency from organisms to ecosystems - definitions, theories, and empirical evidence. Biogeosciences 15, 5929–5949. https://doi.org/10.5194/bg-15-5929-2018.

Manzoni, S., Chakrawal, A., Spohn, M., Lindahl, B.D., 2021. Modeling microbial adaptations to nutrient limitation during litter decomposition. Frontiers in Forests and Global Change 4. https://doi.org/10.3389/ffgc.2021.686945.

Marx, M.-C., Wood, M., Jarvis, S., 2001. A microplate fluorimetric assay for the study of enzyme diversity in soils. Soil Biology and Biochemistry 33, 1633–1640. https://doi.org/10.1016/S0038-0717(01)00079-7.

Mason-Jones, K., Breidenbach, A., Dyckmans, J., Banfield, C.C., Dippold, M.A., 2023. Intracellular carbon storage by microorganisms is an overlooked pathway of biomass growth. Nature Communications 14. https://doi.org/10.1038/s41467-023-37713-4.

Moorhead, D.L., Sinsabaugh, R., 2006. A theoretical model of litter decay and microbial interaction. Ecological Monographs 76, 151–174. https://doi.org/10.1890/0012-9615(2006)076[0151:ATMOLD]2.0.CO;2.

Mooshammer, M., Wanek, W., Hämmerle, I., Fuchslueger, L., Hofhansl, F., Knoltsch, A., Schnecker, J., Takriti, M., Watzka, M., Wild, B., Keiblinger, K.M., Zechmeister-Boltenstern, S., Richter, A., 2014. Adjustment of microbial nitrogen use efficiency to carbon:Nitrogen imbalances regulates soil nitrogen cycling. Nature Communications 5, 1–7. https://doi.org/10.1038/ncomms4694.

Nordgren, A., 1988. Apparatus for the continuous, long-term monitoring of soil respiration rate in large numbers of samples. Soil Biology and Biochemistry 20, 955–957. https://doi.org/10.1016/0038-0717(88)90110-1.

Ramin, K.I., Allison, S.D., 2019. Bacterial tradeoffs in growth rate and extracellular enzymes. Frontiers in Microbiology 10. https://doi.org/10.3389/fmicb.2019.02956.

Renella, G., Szukics, U., Landi, L., Nannipieri, P., 2007. Quantitative assessment of hydrolase production and persistence in soil. Biology and Fertility of Soils 44, 321–329. https://doi.org/10.1007/s00374-007-0208-8.

Ropelewska, E., Zapotoczny, P., Dziejowski, J., 2016. An evaluation of cellobiose as an alternative reference substance for isothermal microcalorimetry measurements of soil microbial activity. Thermochimica Acta 623, 102–106. https://doi.org/10.1016/j.tca.2015.11.001.

Russell, J.B., Cook, G.M., 1995. Energetics of bacterial growth: balance of anabolic and catabolic reactions. Microbiological Reviews 59, 48–62. https://doi.org/10.1128/mr.59.1.48-62.1995.

Sandler, S.I., Orbey, H., 1991. On the thermodynamics of microbial growth processes. Biotechnology and Bioengineering 38, 697–718. https://doi.org/10.1002/bit.260380704.

Schimel, J.P., Weintraub, M.N., 2003. The implications of exoenzyme activity on microbial carbon and nitrogen limitation in soil: a theoretical model. Soil Biology and Biochemistry 35, 549–563. https://doi.org/10.1016/S0038-0717(03)00015-4.

Sinnott, M.L., 1998. The Cellobiohydrolases of Trichoderma Reesei: a Review of Indirect and Direct Evidence that Their Function Is Not Just Glycosidic Bond Hydrolysis.

Sinsabaugh, R., Manzoni, S., Moorhead, D.L., Richter, A., 2013. Carbon use efficiency of microbial communities: stoichiometry, methodology and modelling. Ecology Letters. https://doi.org/10.1111/ele.12113.

Sørensen, T.H., Cruys-Bagger, N., Borch, K., Westh, P., 2015. Free energy diagram for the heterogeneous enzymatic hydrolysis of glycosidic bonds in cellulose. Journal of Biological Chemistry 290, 22203–22211. https://doi.org/10.1074/jbc.M115.659656.

Tewari, Y.B., Goldberg, R.N., 1989. Thermodynamics of hydrolysis of disaccharides. Journal of Biological Chemistry 264, 3966–3971. https://doi.org/10.1016/S0021-9258(19)84947-5.

Tewari, Y.B., Lang, B.E., Decker, S.R., Goldberg, R.N., 2008. Thermodynamics of the hydrolysis reactions of 1,4-β-d-xylobiose, 1,4-β-d-xylotriose, d-cellobiose, and d-maltose. Journal of Chemical Thermodynamics 40, 1517–1526. https://doi.org/10.1016/j.jct.2008.05.015.

Trapp, S., Brock, A.L., Nowak, K., Kästner, M., 2018. Prediction of the formation of biogenic nonextractable residues during degradation of environmental chemicals from biomass yields. Environmental Science and Technology 52, 663–672. https://doi.org/10.1021/acs.est.7b04275.

Voet, D., Voet, J.G., 2010. Biochemistry, fourth ed. John Wiley & Sons, John Wiley & Sons.

Wadsö, I., 2009. Characterization of microbial activity in soil by use of isothermal microcalorimetry. Journal of Thermal Analysis and Calorimetry 95, 843–850. https://doi.org/10.1007/s10973-008-9467-3.

Wadsö, I., 1995. Microcalorimetric techniques for characterization of living cellular systems. Will there be any important practical applications? Thermochimica Acta 269–270, 337–350. https://doi.org/10.1016/0040-6031(95)02673-8.

Wang, C., Kuzyakov, Y., 2023. Energy use efficiency of soil microorganisms: driven by carbon recycling and reduction. Global Change Biology. https://doi.org/10.1111/gcb.16925.

Wilson, D.B., 2008. Three microbial strategies for plant cell wall degradation. In: Annals of the New York Academy of Sciences. Blackwell Publishing Inc., pp. 289–297. https://doi.org/10.1196/annals.1419.026

Wirsching, J., Endress, M.G., Di Lodovico, E., Blagodatsky, S., Fricke, C., Lorenz, M., Marhan, S., Kandeler, E., Poll, C., 2025. Coupling energy balance and carbon flux during cellulose degradation in arable soils. Soil Biology and Biochemistry 202. https://doi.org/10.1016/j.soilbio.2024.109691.

Yan, S., Wu, G., 2013. Secretory pathway of cellulase: a mini-review. Biotechnology for Biofuels 6, 177. https://doi.org/10.1186/1754-6834-6-177.

Zheng, Q., Hu, Y., Zhang, S., Noll, L., Böckle, T., Richter, A., Wanek, W., 2019. Growth explains microbial carbon use efficiency across soils differing in land use and geology. Soil Biology and Biochemistry 128, 45–55. https://doi.org/10.1016/j.soilbio.2018.10.006.